

Review

The Symmetric Active Site of Enantiospecific Enzymes

Elena Rosini , Loredano Pollegioni  and Gianluca Molla * 

“The Protein Factory 2.0”, Department of Biotechnology and Life Sciences (DBSV), University of Insubria, Via Dunant 3, 21100 Varese, Italy; elena.rosini@uninsubria.it (E.R.); loredano.pollegioni@uninsubria.it (L.P.)

* Correspondence: gianluca.molla@uninsubria.it

Abstract: Biomolecules are frequently chiral compounds, existing in enantiomeric forms. Amino acids represent a meaningful example of chiral biological molecules. Both L- and D-amino acids play key roles in the biochemical structure and metabolic processes of living organisms, from bacteria to mammals. In this review, we explore the enantiospecific interaction between proteins and chiral amino acids, introducing theoretical models and describing the molecular basis of the ability of some of the most important enzymes involved in the metabolism of amino acids (i.e., amino acid oxidases, dehydrogenases, and aminotransferases) to discriminate the opposite enantiomers. Our analysis showcases the power of natural evolution in shaping biological processes. Accordingly, the importance of amino acids spurred nature to evolve strictly enantioselective enzymes both through divergent evolution, starting from a common ancestral protein, or through convergent evolution, starting from different scaffolds: intriguingly, the active sites of these enzymes are frequently related by a mirror symmetry.

Keywords: enantioselectivity; chirality; D-amino acids; aminotransferases; amino acid oxidases; dehydrogenases; active site



Citation: Rosini, E.; Pollegioni, L.; Molla, G. The Symmetric Active Site of Enantiospecific Enzymes. *Symmetry* **2023**, *15*, 1017. <https://doi.org/10.3390/sym15051017>

Academic Editors: John H. Graham and Chris Bishop

Received: 5 April 2023

Revised: 27 April 2023

Accepted: 28 April 2023

Published: 2 May 2023



Copyright: © 2023 by the authors. Licensee MDPI, Basel, Switzerland. This article is an open access article distributed under the terms and conditions of the Creative Commons Attribution (CC BY) license (<https://creativecommons.org/licenses/by/4.0/>).

1. Introduction

Chirality is a concept introduced by Louis Pasteur in 1848 through his seminal work on tartaric acid [1,2]. As he stated in 1874: “*The universe is asymmetric and I am persuaded that life, as it is known to us, is a direct result of the asymmetry of the universe or of its indirect consequences.*”. Amino acids, carbohydrates, and several lipids are “chiral” compounds; they exist as two identical molecules that use the space differently since, like our hands, they are mirror images. These chiral compounds are the precursors of several polymers containing chiral centres (i.e., proteins, DNA, RNA, and polysaccharides). In addition, many cellular metabolites also contain chiral centres, and, in most cases, one specific configuration is preferred.

In nature, there are about 500 amino acids, but only 20 are proteogenic (i.e., they can be found in proteins). Amino acids represent a well-known example of chiral biological molecules. A typical α -amino acid possesses a central carbon atom (α C, a carbon atom with an sp^3 hybridization) linked to four different substituents: (i) an α -amino (NH_2) and (ii) α -carboxylic group ($COOH$), which at physiological pH are positively and negatively charged, respectively; (iii) an organic group named side chain (there are 20 different side chains in proteogenic amino acids, each possessing a specific size, charge, and polarity); (iv) a hydrogen atom (the α H) (Figure 1A). Of these α -amino acids, glycine is achiral and the other 19 have a chiral carbon and thus exist as either of two possible stereoisomers indicated as enantiomers. The enantiomers of a given compound have identical chemical and physical properties, with the only exception of the mode of interaction with other chiral compounds and with polarized light. For glyceraldehyde, the enantiomer that rotates clockwise (to the right) the plane of polarized light is identified as dextrorotatory (D), while the one that rotates counter-clockwise (to the left) the plane of polarized light is laevorotatory (L). The absolute configurations of simple amino acids and sugars are thus

specified by the L- and D-systems based on the absolute configuration proposed by Emil Fischer for glyceraldehyde [3].

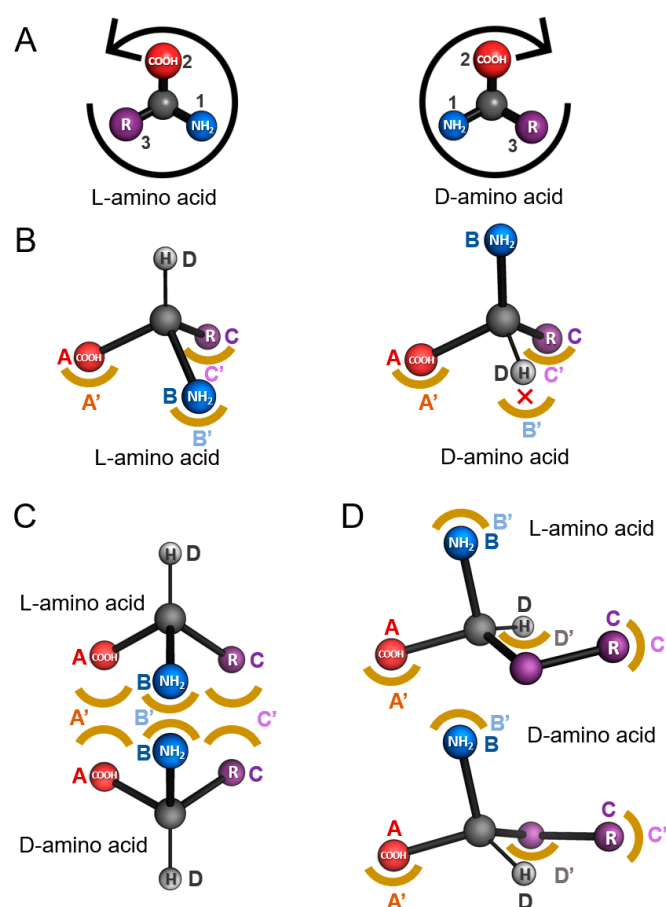


Figure 1. Models for the stereoselective discrimination of enantiomers of amino acids. (A) Absolute configuration of an L- and D-amino acid. The α H (priority 4), which points away from the point of view, is hidden behind the α C. Groups attached to the α C are numbered accordingly to their priority. (B) The “3-contact point model”: the enantiomer on the right can form only two out of three correct interactions (the D-B' mismatch is indicated by a red X). (C) The “4-contact point model” (“mirror image model”): in this enantiomeric model, three interactions between the two enantiomers and the protein, are conserved, while the fourth “functional direction” (D) points toward opposite directions. This model is also named the “umbrella-like” model because the mirror image of the enantiomers is similar to a molecule that has been subjected to a Walden inversion. (D) The “enantiomer superposition model”: the chiral centre and the substituent groups A and B are coplanar; both enantiomers of the amino acid can interact with the protein groups A', B', and C'. Specifically, the flexibility of the side chain allows the conservation of the C-C' interaction between the two enantiomers and the enzyme.

The ubiquity of L-amino acids in proteins and of D-sugars in nucleic acids strongly suggests that these choices were fixed prior to the appearance of the last universal common ancestor (LUCA). On the other hand, the use of both enantiomers of chiral phospholipids occurred post-LUCA since archaea and bacteria use opposite enantiomers [4]. Among the main outstanding questions about the origins of life [5] is the reason that led to the transition from racemic, abiotic chemistry to the homochirality observed in biology, and whether this transition was a biological invention or was started by abiotic processes. Although it is still elusive as to why and how only L-amino acids were selected for peptide/protein synthesis during the prebiotic era, D-amino acids have been retained within the biological systems and are implicated in important biological processes.

D-amino acids are the main component of the bacterial cell wall, as well as of several antibiotics [6–9]. These compounds are also present at high concentrations in plants, invertebrates, and mammals, where they fulfil specific and different biological functions. In the mammalian brain, D-serine (D-Ser) acts as a co-agonist of the *N*-methyl-D-aspartate (NMDA)-type glutamate receptors, responsible for learning and memory, and the alteration of its level has been related to psychiatric and neurodegenerative disorders [10,11]. D-aspartate (D-Asp) is a main regulator of adult neurogenesis and plays an important role in the development of endocrine functions [12]. Furthermore, foods also contain D-amino acids, naturally originated or processing-induced [13].

Chiral amino acids are also largely used in different industrial sectors, such as the pharmaceutical, cosmetic, food, agricultural, and feedstuff industries [14–16]. The impressive number of applications of chiral amino acids has stimulated a great deal of innovation in synthetic methodologies for their preparation, especially employing stereospecific enzymes under mild conditions [17]. On this side, most protein binding sites are chiral and able to preferentially bind a specific enantiomer of a chiral ligand. Several enzymes show a strict enantiospecificity toward substrates both in the binding process (the physical step of catalysis) and/or in the catalytic step (the chemical step of catalysis). This aspect must be considered when designing specific pharmaceutical drugs. The different types of stereoselective metabolism could bear important consequences on several aspects of their pharmacokinetics and pharmacodynamics [18–20]. In recent years, the discovery that the pharmacologically inactive stereoisomer in a racemate could be potentially toxic pushed the major drug regulatory agencies to issue specific guidelines for the development and use of chiral molecules as drugs [12].

In this review, we aim to rationalize the molecular arrangements employed by different stereospecific enzymes able to distinguish between L- and D-amino acid enantiomers, thus providing selected examples of enantioselectivity in oxidases, dehydrogenases, and aminotransferases.

2. Models of Enantiospecificity in Protein-Ligand Interaction

The first model for the stereospecific discrimination of ligands was proposed by Easson in 1933 [21]. This model was subsequently further refined to account for more complex enantiospecific situations [22,23]. All the proposed models are based on the concept of a point of interaction between a specific atom or chemical group of the ligand and a corresponding atom or chemical group of the protein. These ligand–protein interactions are called “attachment” or “contact” points. Additional factors that could play a key role in the enantiospecificity of enzymes (e.g., protein conformational changes, enantioselective access to the active site) will not be discussed in the present review because they represent specific situations and have not yet been extensively investigated. The original model (Easson–Stedman model) was based on three attachment points (“3-contact point model”, Figure 1B). Three binding determinants of the ligand (A, B, and C) interact with three corresponding groups on the enzyme (A', B', and C'), all laying on the same plane [21]. Therefore, provided that the substrate can usually bind to the attachment points from a single direction, binding the “wrong” enantiomer would result in a single mismatch (Figure 1B).

The ability of several enzymes (e.g., D-amino acid oxidases, DAAOs, or L-amino acid oxidases, LAAOs) to bind both enantiomers of specific substrates, even if they retain the ability to catalyse the chemical reaction of a single enantiomer, questioned this model. More recently, a new model has been proposed [23,24]: similar to the previous one, the chiral ligand interacts with the binding site through three planar contact points (A, B, and C and A', B', and C', for the ligand and the protein, respectively). In addition, in order for the reaction to happen, the fourth substituent of the chiral centre of the ligand (D) should point toward a specific position of the active site (D'). According to this model, in principle, the protein should be able to bind both enantiomers of the substrate with the substituent (D) pointing in opposite directions with respect to the chiral centre. An implicit consequence

of this model is that there should be enough space at the opposite region of the active site to accommodate the substituent (D) in the two potential orientations. Therefore, this kind of enantiospecificity is usually observed when the (D) substituent is small; examples of enzymes that show this model are amino acid oxidases (AAOs). This model is named as the “4-contact point model” (Figure 1C) or the “mirror-image packing model” since the three binding determinants (A' , B' , C') define a symmetry plane of a pseudo-specular symmetry [25].

A third model, proposed by Bentley and colleagues, is a variant of the “3-contact point model”. This model has been observed in isocitrate dehydrogenase (EC 1.1.1.42), a key enzyme in the tricarboxylic acid cycle that converts threo-D₅-isocitrate to 2-oxoglutarate and CO₂ [26]. It requires that the attachment sites on the protein should not be coplanar and that one of the substituents of the substrate chiral centre possesses a certain structural “flexibility” (at least two degrees of freedom). This model can be applied to the binding of substrates such as phenylalanine. The presence of a -CH₂- group between the α C and the benzene side chain allows the latter to interact with the same binding determinant at the enzyme active site (i.e., C' in Figure 1D) in both the L- and D-enantiomers. This model is referred to as the “enantiomer superposition model”. One of the main differences between the “mirror-image packing” and the “enantiomer superposition” models is the reciprocal orientation of the fourth substituent (D), usually a H atom between the two enantiomers. The (D) substituent is oriented in opposite directions in the “mirror-image packing model”, whereas, in the “enantiomer superposition model”, it will show an angle of $\sim 109^\circ$ (i.e., the bond angle observed in sp³ hybridization) with respect to the position observed in the other enantiomer.

Recently, enzyme enantiospecificity has been also studied using bioinformatic approaches, such as quantum chemical simulations which are based on transition state modelling and density functional theory and correlate the enzyme enantiospecificity to the predicted transition state energies of the reaction steps. These approaches highlighted that the enantiospecificity of enzymes does not necessarily correlate with the enzyme–substrate or enzyme–intermediate complex formation, as stated in the canonical models discussed above. Indeed, the enantiospecificity-determining transition state(s) can be located in a part of the reaction different from the binding step. Thus, in order to correctly identify these steps, the entire reaction mechanism should be explored [27]. The quantum chemical methods also allow the correlation of the altered enantiospecificity in mutated enzymatic pathways to cancer biology. This approach was used to identify the rationale of the altered enantiospecificity of a mutated isocitrate dehydrogenase: in specific cancer cell lines, the variant enzyme produced only D-2-hydroxyglutarate instead of the L- enantiomer [28].

3. Enantiospecificity in Amino Acid Oxidases and Dehydrogenases

Amino acid oxidases and dehydrogenases (AAOs and AADHs) catalyse the strictly stereospecific oxidative deamination of the L- or D-enantiomers of amino acids. During the reaction, the substrate amino acid is oxidized with the production of the corresponding imino acid which, in aqueous solution, spontaneously deaminates producing the corresponding α -keto acid and ammonia. In AAOs, the reduced cofactor (flavin adenine mono or dinucleotide, FMNH₂ or FADH₂, respectively) is reoxidized by a molecular oxygen molecule producing hydrogen peroxide (Figure 2A,B). On the other hand, in AADHs, the electrons deriving from the amino acid oxidation are transferred through the reduced cofactors FADH₂ or nicotinamide adenine dinucleotide (phosphate), NAD(P)H, to a membrane-associated electron acceptor (usually a molecule belonging to the coenzyme Q family) [29,30]. This electron transfer/reoxidation system allows AADHs to perform the oxidative deamination of amino acids even under anaerobic conditions.

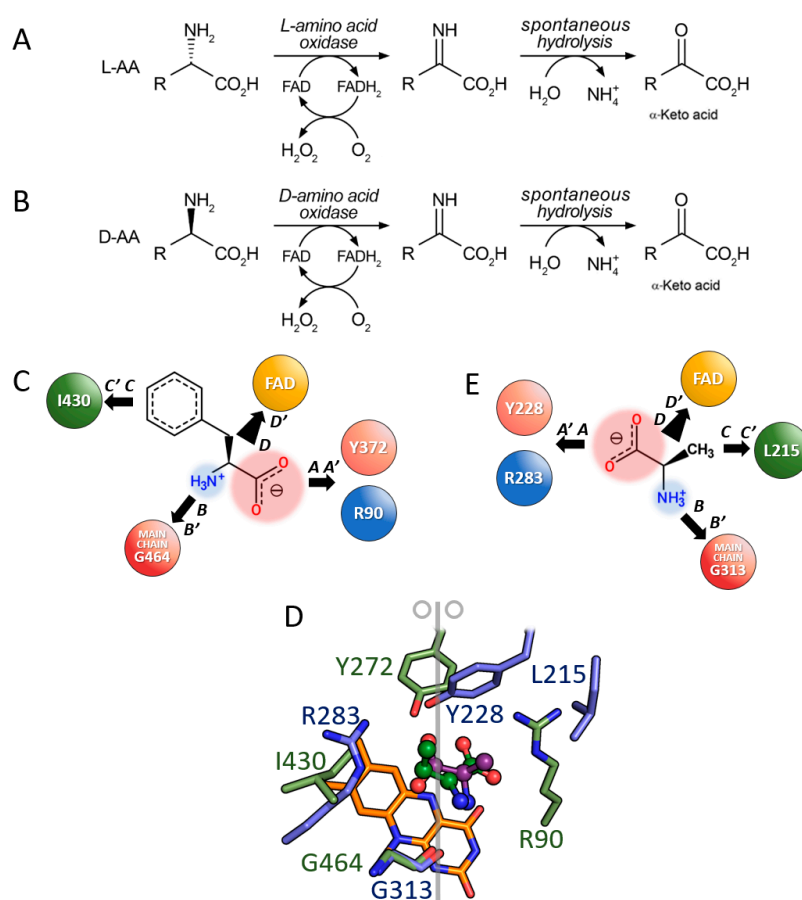


Figure 2. Symmetric arrangement of the active site of DAAO and LAAO. (A) Reaction catalysed by LAAO and (B) by DAAO. (C) Scheme of the active site of *Calloselasma rhodostoma* LAAO (CrLAAO) in complex with L-Phe (PDB code 2IID). (D) Superimposition of the structure of CrLAAO (green) and human DAAO (hDAAO, blue) with bound L-Phe (the benzene ring of the side chain is not shown) and D-alanine (modelled based on the structure of hDAAO in complex with iminoserine, PDB code 2E49), respectively. The vertical grey line represents the symmetry axis perpendicular to the FAD isoalloxazine ring. (E) Scheme of the active site of hDAAO in complex with D-alanine. Only the residues responsible for the main substrate-protein interactions are represented.

According to their strict enantiospecificity, AAOs and AADHs can be divided into two main groups. The first group is composed of enzymes active on L-amino acids. L-amino acid oxidases (EC 1.4.3.2, LAAOs) are the most abundant components of this group. LAAOs can be in turn divided into enzymes possessing a wide substrate specificity (e.g., LAAO from the bacterium *Rhodococcus opacus* and LAAOs from vertebrates) and enzymes showing a narrow substrate preference (e.g., L-aspartate oxidase, L-glutamate oxidase, L-lysine oxidase) [31]. Interestingly, L-lysine ϵ -oxidase (LodA, EC 1.4.3.20) and its homologous GoxA, active on glycine, produced by the marine bacterium *Marinomonas mediterranea* also belong to this group [32,33]. This latter enzyme possesses the peculiar cysteine tryptophylquinone cofactor (CTQ), a type of quinone cofactor generated by the post-translational modification of two residues belonging to the same protein chain. Finally, this group also includes bacterial L-amino acid dehydrogenases (LAADHs, EC 1.4.1.5) [34].

The other side of the AAOs and AADHs mirror is occupied by enzymes active on the D-enantiomer of amino acids: the most important group is formed by D-amino acid oxidases (DAAOs, EC 1.4.3.3), ubiquitous flavoproteins present in almost all eukaryotes (with the exception of plants). The DAAO from pig kidney was the first described AAO in 1935 [35] and represents the prototype of the FAD-dependent oxidase family [36,37]. Additionally, D-aspartate oxidase (DASPO or DDO, EC 1.4.3.1) and bacterial D-amino acid

dehydrogenases (DAADHs, EC 1.4.99.1) belong to this second group. Interestingly, the non-enantiomeric enzyme glycine oxidase from *Bacillus subtilis*, which is mainly active on the non-chiral amino acid glycine, can be classified in this group because of its low, but not marginal, activity on D-amino acids (e.g., D-alanine, D-Ala, and D-proline, D-Pro) [33,38,39] and large structural similarity with DAAO [40,41].

3.1. Comparison between D- and L-Amino Acid Oxidases

LAAOs and DAAOs are FAD-containing flavoenzymes whose catalytic mechanism proceeds through the partial superimposition of the molecular orbitals of the atoms involved in the reaction, which is the highest occupied molecular orbital (HOMO) of the substrate α H and the lowest unoccupied molecular orbital (LUMO) of the FAD cofactor N(5) (the so-called orbital steering mechanism). Interestingly, the amino acid functional groups of the active site are not involved in the chemical step of catalysis, but they play a fundamental role in the recognition, binding, and orientation of the substrate [42–44].

The LAAO activity is widely distributed in nature, from bacteria [45,46] to mammals, which express LAAO in several tissues (e.g., in liver, kidney, brain, mammary gland, and polymorphonuclear leukocytes). In particular, snake venom represents the source of the best-characterized LAAOs [47,48]. Despite the low sequence identity between different LAAOs (e.g., the LAAO from the snake *Crotalus adamanteus*, CrLAAO, shares less than 23% sequence identity with the one from the bacterium *Rhodococcus opacus*), their overall fold is very similar, with a root mean squared deviation (RMSD) of ~ 1.0 – 1.2 Å when superimposed [31,47]. Indeed, most of the differences are gathered in protein regions that are either removed during maturation or form surface loops; only marginal alterations have been observed in regions close to the substrate binding site. The high similarity of the overall three-dimensional fold and the very similar active site geometry support a strong evolutionary relationship among these enzymes [31]. The physiological role of LAAOs is often connected to their ability to generate hydrogen peroxide [48], a potent antimicrobial agent that can play an important role in microbial competition processes [49], biofilms dynamics [50], the protection of the fish skin from bacterial infections [51], and human immune system response [52,53]. Finally, LAAOs are also interesting for their potential biocatalytic applications [31].

Bacterial and eukaryotic LAAOs share the same mode of substrate binding; the substrate is bound at the active site on the *re*-face of the isoalloxazine moiety of FAD. The ability of LAAOs to discriminate between the two enantiomers of the amino acids can be explained based on the “4-contact point model” (Figure 1C). In agreement with this model, the architecture of the enzyme active site is arranged so that three directional binding interactions (attachment sites) and one “functional direction” between the substrate and the active site can be identified [23]. The major anchor point (A-A') is represented by a salt bridge interaction between the α -carboxylic group of the amino acid (negatively charged) and the positively charged guanidinium group of arginine of the active site (Arg90 in CrLAAO), which is located close to the pyrimidine side of the isoalloxazine (Figure 2D). This interaction is strengthened by additional hydrogen bonds between the oxygen atoms of the α -carboxylate and the hydroxyl of Tyr372, the N(5) atom of the flavin, and an active site water molecule. This latter molecule plays an important role during catalysis since it can act as a H^+ donor for the activation of O_2 during the re-oxidation of $FADH_2$ [54]. The second anchor point (B-B') is a hydrogen bond between the α -amino group of the substrate and the main chain C=O of Gly464 and to a second active site water molecule. The third anchor point (C-C') is represented by the upper region of the active site which accommodates the substrate side chain and is central for the determination of the substrate scope in LAAOs. Most of the active site differences among members of this family cluster in this region. The “functional” direction (D-D') is represented by the α H that points towards the flavin N(5) allowing an efficient hydride transfer during catalysis.

Additionally, in DAAOs, the substrate D-amino acid is bound at the *re*-face of the isoalloxazine moiety [42,55]. The residue that mainly contributes to the binding energy

of the substrate (interaction A-A') is Arg283 (residue numbering refers to the human enzyme, hDAAO), which forms an electrostatic interaction with the negatively charged α -carboxyl group of the amino acid [56]. The same group is bound through a H-bond to the hydroxyl side chain of Tyr228. Due to the relevant contribution to substrate binding, these two residues are conserved in all DAAOs and DASPOs. The α -amino group of the substrate forms two H-bonds with the main chain oxygen of Gly313 and with the oxygen of the C(4)=O group of FAD (interaction B-B') [57]. In yeast DAAO, the α -amino group is also H-bonded to an active site water molecule [42]. As in LAAOs, the third attachment point (C-C') in DAAOs is also formed by various interactions between the substrate side chain and the residues lining a hydrophobic cavity in the upper part of the active site. In hDAAO, this substrate specificity pocket is formed by residues Leu51, Gln53, Leu215, and Ile230. In addition, when aromatic ligands are bound at the active site, they form a stacking interaction with Tyr224 (belonging to the flexible active site loop) [57]. Finally, the "functional direction" (D-D') is also represented by the orientation of the α H in DAAOs (Figure 2E).

The relevance of the interaction formed by the α NH₂ group of the substrate (B-B') in the enantiospecificity of DAAOs has been demonstrated by [58]. When the D-Ala oxidation is performed at pH 9.8, the amino group of the substrate is deprotonated and it becomes an isostere of the side chain CH₃ group; this decreases the strength of the (B-B') interaction and, at the same time, allows to locate the neutral amino group in the hydrophobic substrate specificity pocket (site C). As a consequence, under these conditions, L-alanine (L-Ala) can bind and become a substrate of DAAO. A similar occurrence is also evident with proline, where the groups -CH₂- and -NH- of the pyrrole ring (substituents of the α C) are isosteres, and, as a consequence, both enantiomers of proline can fit the B' and C' sites of the active site of DAAO [58].

The superimposition of the hDAAO structure (PDB code 2E49) to the CrLAAO structure (PDB code 2IID) reveals the mechanism of strict enantioselectivity of these two enzymes acting on "mirror" substrates. Overall, the binding mode observed in LAAOs is similar to the one of DAAOs [36,42,59] with the substrates bounded at the same side of the FAD (*re*-face) and occupying the same region of the active site. On the other hand, because of the opposed enantiospecificity, the arginine (attachment point A) and the specificity binding pocket (attachment point C) appear mirrored (i.e., they are switched). The (B-B') interaction is conserved (Gly313 is superimposed to Gly464) and, in addition, the H-bond between one oxygen of the carbonyl group and the active site tyrosine is also conserved; in the two superimposed enzymes, the hDAAO Tyr228-OH group is at a distance of 1.5 Å from the LAAO Tyr372-OH group. Additionally, the "functional direction" is conserved since the α H of the amino acid points to the N(5) of the flavin at ~3.2–3.4 Å. As a result, the active sites of DAAOs and LAAOs are a mirror of each other with the symmetry plane perpendicular to the plane of the isoalloxazine ring of the cofactor (Figure 2D). It is interesting to highlight that, from an evolutionary point of view, the homologous DAAOs and LAAOs acquired a strict enantiospecificity through limited changes at the active site, among which, the most important one has been the switch of the position of the Arg required for binding the α -carboxyl group of the substrate.

From a functional point of view, the following situations can be envisaged when an L-amino acid substrate is modelled at the active site of DAAO. As we assume that the main interaction (A-A', i.e., the salt bridge between the α -carboxylic group and the arginine) is conserved, only three alternative potential conformations are possible (Figure 3). Each conformation would simultaneously satisfy two out of four anchor points, while the remaining two will be switched (Figure 3, conformations D,E,F). This will inevitably result in steric hindrance issues and/or the loss of stabilizing interactions, that, in turn, will result in a decrease in the binding energy and the probability of the formation of the complex. Indeed, conformation C (Figure 3C) will satisfy the three directions (allowing similar binding energy between the two enantiomers): this conformation entails a slight displacement of the α C and, importantly, a switch of the direction of the α H that points

in the “wrong” direction (i.e., opposite to the FAD cofactor). This prevents the transfer of the hydride ion to FAD during catalysis. Consequently, even if the L-enantiomer of the substrate could bind to the active site, it will not be oxidized by the enzyme. L-lactate (a compound possessing a chemical structure very similar to L-Ala) binds in a not-catalytically competent orientation (Figure 3B) [42], also named the “umbrella-like model” (Figure 1C). In this conformation, the binding energy for the two enantiomers is close (because only one mismatch between the substituents and the binding sites is created). This binding model might explain why several enzymes are active, even if to a different extent, on both the enantiomers of a substrate; in these cases, the two enantiomers are defined as the slow- and fast-reacting enantiomers.

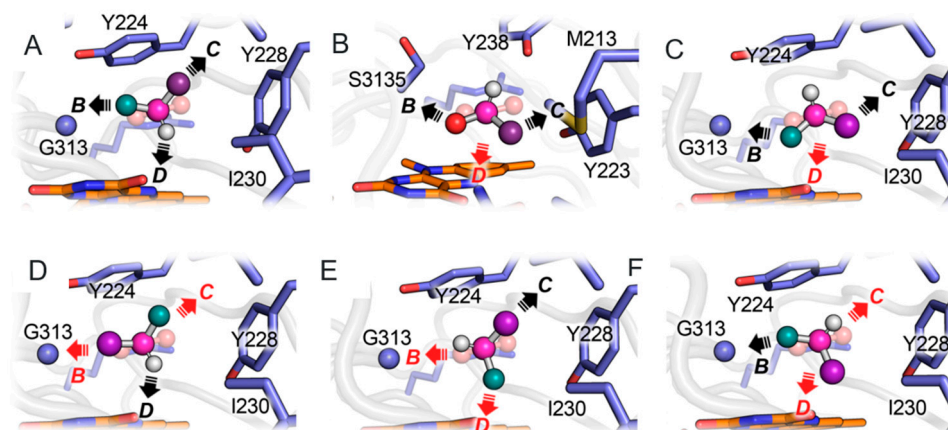


Figure 3. D- and L-enantiomers of alanine and L-lactate bound at the active site of DAAO. (A) D-Ala modelled in the active site of hDAAO (based on the structure of hDAAO in complex with iminoserine, PDB code 2E49). (B) L-lactate in complex with yeast DAAO (PDB code 1C0K). (C) L-Ala modelled at the active site of hDAAO accordingly to the “inverted umbrella model”. (D–F) L-Ala modelled at the active site of hDAAO. The α H, side chain, and α -amino groups are represented as grey, teal, and deep purple spheres, respectively. In all panels, the α COOH (depicted in salmon) is superimposed to the one of D-Ala. The FAD cofactor is shown in orange sticks. Labelled arrows represent the interaction accordingly to the “4-contact point model” (the interaction A between the active site arginine and the carboxylic group of the ligand is not shown); red arrows represent “wrong” interactions.

D-aspartate oxidase (DASPO, EC 1.4.3.1) is a close paralogue of DAAO, with which it shares a high sequence similarity [60,61]. It is able to oxidize D-Asp and, to a lesser extent, D-glutamate (D-Glu), therefore playing a crucial role in the utilization, elimination, and intracellular level regulation of acidic D-amino acids in organisms ranging from bacteria to mammals. In the yeast *Candida humicola*, DASPO allows the microorganism to use D-Asp as a carbon and nitrogen source [62]. In the nematode *C. elegans* (which expresses three different DASPOs), DASPO activities participate in the modulation of the nematode fertility, growth, and lifespan [63]. Importantly, in mammals, this enzyme is a key player in the regulation of the neuromodulator D-Asp in the brain and in the neuroendocrine system [64–66]. The active site of DASPO resembles the one of hDAAO: the main difference concerns the substrate specificity pocket (site D’) which, in DASPO, is positively charged due to the presence of two additional arginines (Arg216 and Arg237) in comparison to hDAAO [64].

While DASPO is a catabolic enzyme, L-aspartate oxidase (LASPO, EC 1.4.3.16), the amino acid oxidase active on L-Asp, is a prokaryotic anabolic enzyme since it catalyses the first step of the de novo synthesis of NAD^+ from L-Asp and dihydroxyacetone phosphate as precursors [67]. In the reaction catalysed by LASPO, the electrons deriving from L-Asp oxidation are transferred to molecular oxygen (as in DAAO) or to fumarate, which is reduced to succinate. This latter reaction is used to foster the tricarboxylic acid cycle in cyanobacteria.

Interestingly, L- and D-aspartate oxidase structures cannot be superimposed since these enzymes are not evolutionary related and belong to different structural families; in agreement with PFAM classification, LASPO domains belong to PF00890—FAD-binding domain—and to PF02910—fumarate reductase flavoprotein C-term—while DASPO, such as DAAO, belongs to PF01266—FAD-dependent oxidoreductase. Indeed, a close inspection of the structure shows that in LASPO, L-Asp is bound in a very peculiar way, i.e., with an orientation that is rotated by 90° in comparison with the one observed in DASPO and DAAO and, also, in comparison with L-amino acids in LAAO and LAAD.

3.2. Comparison between D-Amino Acid Oxidases and L-Amino Acid Deaminases

L-Amino acid deaminase (LAAD) catalyses a reaction similar to LAAO (i.e., the oxidative deamination of L-amino acids). The main difference resides in the FAD cofactor reoxidation step: in LAADs, electrons deriving from the substrate are transferred to a membrane-associated electron acceptor, most likely a cytochrome b, with no production of hydrogen peroxide (Figure 4A) [68].

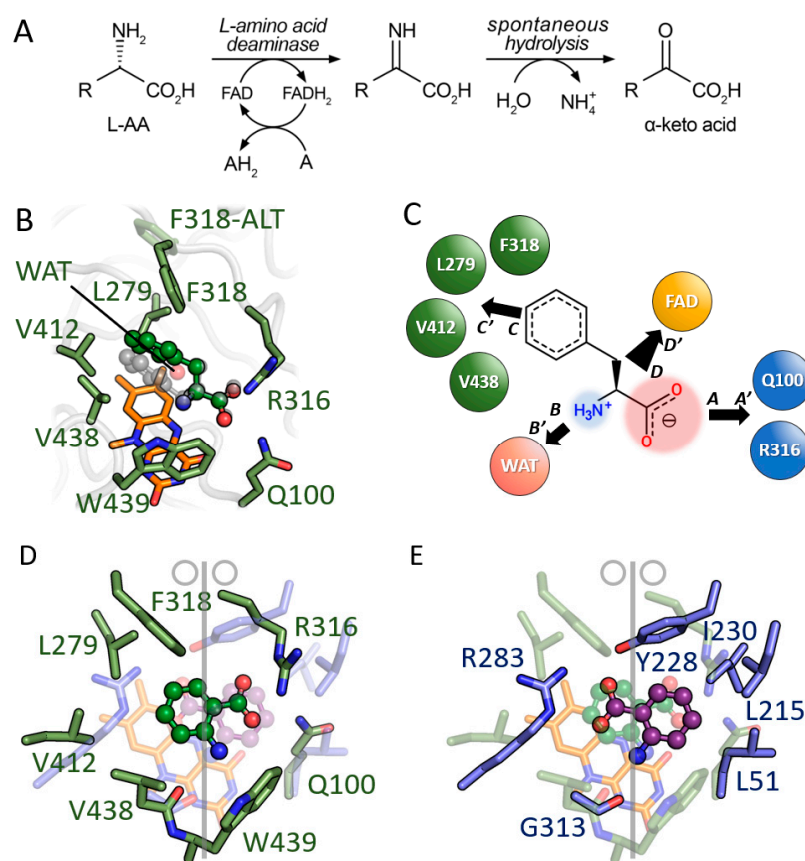


Figure 4. Symmetric arrangement of the active site of LAAD and DAAO (PDB code 2E4A). (A) Reaction catalysed by LAAD. (B) Scheme of the active site of PmaLAAD in complex with L-Phe (green) and D-Phe (grey, transparent). The ligands were modelled based on the structure of PmaLAAD in complex with aminobenzoate (PDB code 5FJN). The side chain of L-Phe is accommodated in the substrate specificity pocket thanks to the flexibility of Phe318. On the other hand, the side chain of D-Phe cannot be accommodated in the same region due to potential steric clash with Val412 and Val438 side chains. (C) Schematic representation of the interactions at the active site of PmaLAAD according to the 4-point binding model. (D) Superimposition of the structure of PmaLAAD (green, solid) and hDAAO (blue, transparent) in complex with the ligand aminobenzoate; only the FAD cofactor (yellow) of PmaLAAD is shown. The vertical grey line represents the symmetry axis perpendicular to the FAD isoalloxazine ring. (E) Same representation as in panel D, with hDAAO solid (blue) and PmaLAAD transparent (green).

LAAD is only expressed by microorganisms belonging to the genus *Proteus*. This microorganism produces two different types of this membrane enzyme (type-I and type-II LAADs), which differ in substrate specificity; type-I LAADs are mainly active on bulky hydrophobic amino acids, while type-II LAADs are active on basic amino acids [69,70]. LAADs share only a marginal sequence similarity with L- or D-amino acid oxidases (13.9 and 16.4%, respectively) [68]. LAADs represent the most promising alternative to LAOs for biotechnological applications since the latter enzyme cannot be efficiently expressed in a recombinant form. For example, LAADs have been proposed as biocatalysts for the production of optically pure D-amino acids through the resolution of D,L-racemic mixtures, as biological components in biosensors for the analytical determination of the concentration of L-amino acids [48,71–77] and even as diagnostic or therapeutic agents [78–80].

As in AAOs, the absolute enantiospecificity of LAADs depends on the specific architecture of their active site which, in analogy with AAOs, can be explained accordingly to the four-location model [23]. Among the three binding interactions and the “functional direction” (Figure 4B,C), the electrostatic interaction between the substrate carboxyl group and the guanidine moiety of the side chain of Arg316 (numbering refers to PmaLAAD) (A-A′) provides the main energetic contribution. In addition, one of the oxygen atoms of the carboxylic group of the substrate is also H-bonded to the side chain of Gln100 and to the C=O(4) atom of the FAD isoalloxazine ring. The amino group of the substrate forms a H-bond with the main-chain C=O of Val438 (B-B′) and with an active site water molecule. The substrate side chain forms several van der Waals interactions with large hydrophobic residues (Leu279, Phe318, Val412, Val438, and Trp439) that form a hydrophobic pocket and determine the substrate scope of the enzyme (C-C′). Interestingly, despite the significant difference in substrate specificity between type-I and type-II LAADs, the volume and polarity of the substrate-specificity pocket are conserved (Figure 4B). The functional “direction” (D-D′) is represented by the α H pointing toward the FAD N(5) atom at a distance $<4 \text{ \AA}$, allowing an efficient hydride transfer during catalysis.

In comparison with DAAO, the main residues involved in substrate binding in the LAAD active site are mirrored through a plane perpendicular to the isoalloxazine ring of FAD which encompasses the C(2) and C(4) atoms of the cofactor, a setup resembling the DAAO/LAO pair [44]. Accordingly, the binding of a D-amino acid (e.g., D-Phe) at the active site of LAAD would result in a steric clash between its aromatic side chain and the FAD isoalloxazine moiety and in the positioning of the positively charged amino group into the apolar substrate specificity pocket [68] (Figure 4B).

3.3. Comparison between D-Amino Acid Oxidases and L-Lactate Cytochrome c Oxidoreductase

The superimposition of the structure of the DAAO from pig kidney (pkDAAO) [36] to the structure of L-lactate cytochrome c oxidoreductase (FCB, EC 1.1.2.3) exemplifies a different way to achieve mirror enantioselectivity between the two enzymes. FCB is a flavin adenine mononucleotide (FMN) containing flavoprotein which oxidizes L-lactate to pyruvate with the transfer of the electrons to the acceptor heme b_2 . The substrate L-lactate is similar to L-Ala (apart from the positive charge on the amino group in the latter). The convergent evolution process generated an active site geometry very similar to the one of DAAO, optimized to perform an efficient hydride transfer from the substrate to the flavin (Figure 5) [81]. As in DAAO, in FCB, the substrate is bound close to the cofactor by a two-point electrostatic interaction with an arginine residue (Arg376) but on the opposite side of the flavin isoalloxazine ring (i.e., on the *si*-face, Figure 5B,C). As a consequence, despite the similar architecture, the active site residues of the two enzymes cannot be superimposed unless a mirror symmetry operation was performed using a mirror plane coincident with the flavin isoalloxazine ring. Following this operation, the corresponding couples of interacting atoms or chemical groups show an RMSD of $\sim 0.9 \text{ \AA}$ (namely, Ala49/198, Tyr228/143, Arg283/376, Gly313/His373, active site water/Tyr254, in pkDAAO and FCB, respectively), Figure 5D. The distance between the reactive atom (α C)

of both substrates and the FAD/FMN N(5) is also similar: 3.3 Å and 3.7 Å for pkDAAO and FCB, respectively.

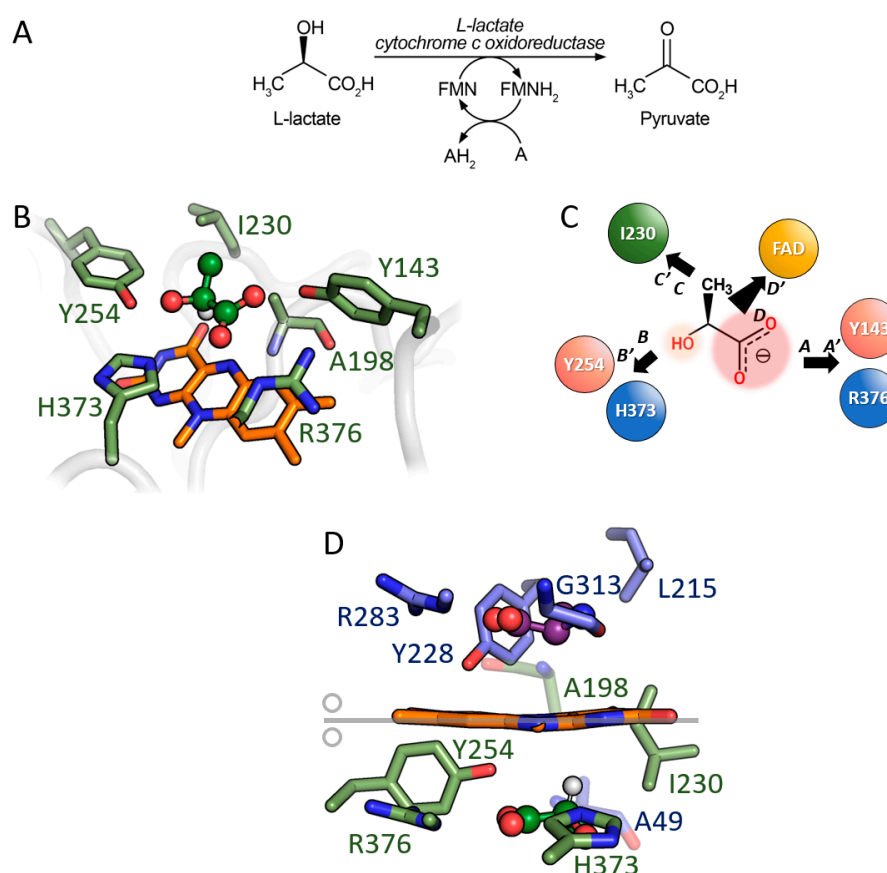


Figure 5. Symmetrical arrangement of the active site of FCB (PDB code 1FCB) and DAAO (PDB code 2E4A). (A) Reaction catalysed by FCB. (B) Active site of FCB in complex with L-lactate (green). (C) Schematic representation of the interactions at the active site of FCB accordingly to the 4-contact point model. (D) Superimposition of the structure of FCB in complex with L-lactate (green) and hDAAO (blue) in complex with D-Ala (blue, modelled based on iminoserine in structure 2E49); only the cofactor FMN (orange) of FCB is shown. The horizontal grey line represents the symmetry axis coincident with the FAD isoalloxazine ring.

The mirror symmetry arrangement of the substrates in the two enzymes follows a precise functional requirement allowing the use of the same mode of binding and catalysis on enantiomerically opposite substrates. The opposite enantiospecificity has been achieved by placing the substrate on the opposite side of the cofactor: D-amino acid is on the *re*-face of the flavin while L-lactate is bound on the *si*-face in DAAO and FCB, respectively (Figure 5). This results in active sites that can be described as mirror images of each other. Thus, the evolutionary unrelated DAAO and FCB represent a remarkable example of a convergent molecular evolution toward common and enantiomeric active site architecture well suited to efficiently catalyse the same reaction (oxidation of an α -amino acid or of an α -hydroxy acid) on substrates with opposite chirality.

3.4. Comparison between D- and L-Amino Acid Dehydrogenases

L-amino acid dehydrogenases (LAADH, EC 1.4.1.X) are membrane-bound bacterial enzymes. The LAADH superfamily contains glutamate (GluDH), valine (ValDH), leucine (LeuDH), phenylalanine (PheDH), and tryptophan dehydrogenase (TrpDH) [82–84]. Although the reaction catalysed by these enzymes is similar to the one of LAAD, the equilibrium of the reactions is shifted toward the reductive amination [85]. LAADHs are very

attractive for the synthesis of chiral compounds such as amines, amino acids, and amino alcohols [86]. As most NADP-dependent dehydrogenases, these enzymes consist of a cofactor-binding domain and a substrate-binding domain, connected through a hinge sequence. The active site is placed in a deep cleft between the two domains [87]. GluDH plays a role in ammonia anabolism catalysing the conversion of 2-oxoglutarate (2-OG) to Glu in a multistep reaction that involves the nucleophilic attack of ammonium to the α -carbon of 2-OG, the elimination of the hydroxyl group from the same carbon and, eventually, the reduction (NAPDH dependent) of the iminoglutamate to L-Glu [88]. In this enzyme, the substrate is bound at the active site through two Lys residues (Lys92 and Lys116) which interact with the γ - and α -carboxylate, respectively, of the 2-OG or L-Glu ligands, as per Figure 6C. During catalysis, residues Lys128 and Asp168 act as an acid and base, respectively, promoting the nucleophilic attack of the ammonium ion to the α -carbon of 2-OG. The same residues switch their role in the second half of the catalytic cycle (i.e., the oxidation of iminoglutamate) [86].

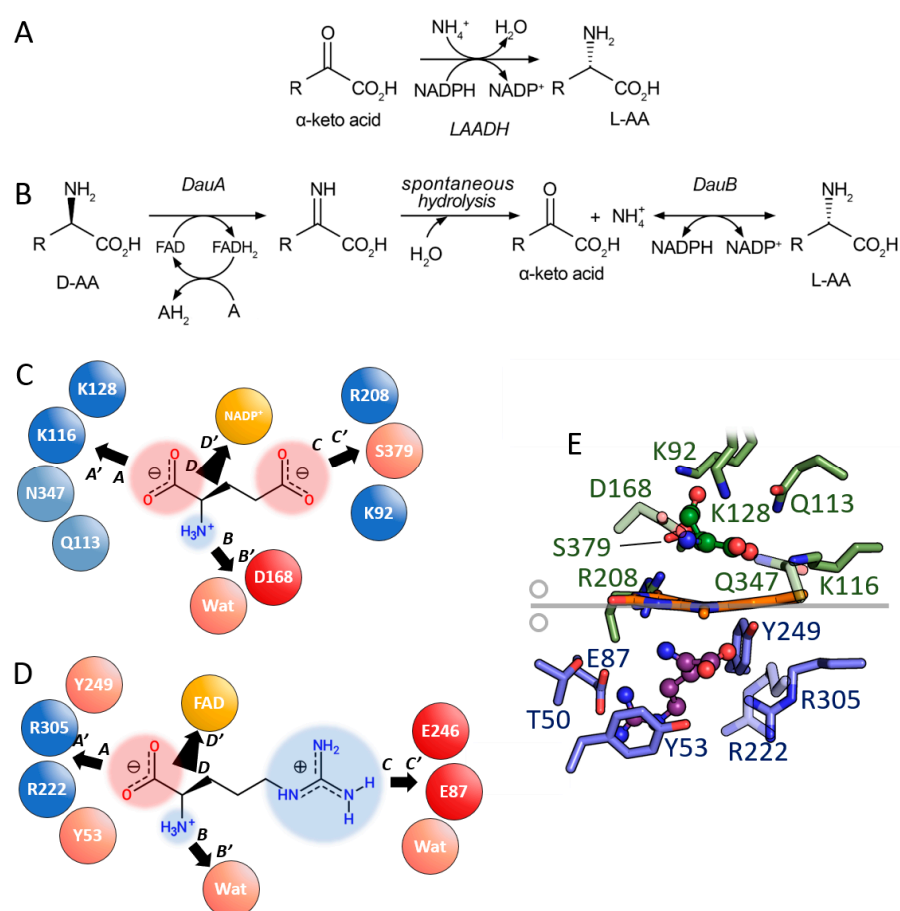


Figure 6. Symmetric arrangement of the active site of LAADHs (PDB code 5GUD) and DAADHs (PDB code 3NYE). (A) Reaction catalysed by glutamate dehydrogenase (GluDH) and by (B) the DauA/DauB pair. (C) Schematic representation of the interactions at the active site of GluDH in complex with glutamate (based on the structure 5GUD) accordingly to the “4-contact point model”. (D) Schematic representation of the interactions at the active site of D-arginine dehydrogenase (DauA or DADH) in complex with L-Arg (based on the structure of PDB code 3NYE). (E) Superimposition of the structure of GluDH (green) and DADH (blue). The nicotinamide ring of NADP⁺ of GluDH has been superimposed on the isoalloxazine ring of FAD (orange) of DADH. The grey horizontal line represents the symmetry axis coincident with the FAD isoalloxazine ring.

D-amino acid dehydrogenases (DAADHs, DADH or DADs, EC 1.4.99.1) are enzymes mainly involved in the metabolization (even under anaerobic conditions) of D-amino

acids [89,90]. For example, a DAADH had been recently identified in *P. mirabilis* [91], a microorganism already known to produce two LAADs [70]. This enzyme allows bacteria to grow on D-amino acids as the sole nutrient source. In addition, it prevents the local over-accumulation of D-amino acids, which generate specific inhibitory effects on bacterial growth [43]. In *Pseudomonas aeruginosa*, a D-Arg dehydrogenase (DauA or DADH) is a component of a dual-enzyme system (DauA/DauB) that catalyses the two-step stereoinversion of D-Arg to L-Arg through the formation of the 2-ketoarginine intermediate (Figure 6B). Thus, the DauA/DauB system allows *P. aeruginosa* to use D-Arg through the bacterial L-arginine catabolic pathways [30]. The first component (DADH) is a flavoprotein which shows the general fold of DAAOs/LAAOs while the second component (DauB) can use both NADPH and NADH as reducing agents [30]. The mode of substrate binding in DADH is very similar to the one of DAAO, Figure 6D: D-Arg is bound next to the FAD *re*-face with the α -carboxylate involved in ionic interactions with two arginines (Arg222 and Arg305, corresponding to Arg283 in hDAAO) and in a H-bond with Tyr53 and Tyr249 (Tyr224 and Tyr228 in hDAAO) (interaction A-A'). The α -amino group is bound to Gly332 (Gly313 in hDAAO) (interaction B-B'). The main difference is the ionic interaction between the positive guanidinium group of the substrate and a glutamate side chain (Glu87) [55] (interaction C-C') since in the corresponding position, the hydrophobic Leu215 is present in hDAAO [57]. As in mammalian DAAO [92], a flexible loop at the active site of DADH is fundamental for the correct binding of the substrate [93].

In *E. coli*, D-alanine dehydrogenase is associated with the cellular membrane and allows the conversion of D-Ala to pyruvate for the production of energy and carbon atoms. Indeed, the electrons produced in this oxidative reaction are transferred through FAD and an iron–sulfur centre to the respiratory chain. The possible acceptor should be a coenzyme Q molecule and, eventually, a cytochrome b_1 [90].

Given the high evolutionary, structural, and functional heterogeneity among LAADHs and DAADHs, a direct comparison between their active site is not obvious. Moreover, at a closer inspection, their enantiospecificity can be explained according to the “3-contact point model” (as in the DAAO/FCB pair), i.e., by a mirror-symmetric arrangement of the substrates in the active site of the two enzymes with the mirror plane coincident with the planar ring(s) of the cofactors. In LAADH, the L-amino acid is located on the *si*-face of the nicotinamide ring of NADP⁺, at a distance and orientation ideal for the hydride transfer of the α H of the substrate to the position (4) of the cofactor ring. In DAADH, the substrate is on the *re*-face of the flavin (Figure 6E) resulting in a mirror image of the LAADH active site. Thus, again, the geometry of the LAADH and DAADH active sites represents an example of convergent molecular evolution for the optimization of a similar catalytic strategy.

4. Aminotransferases

Aminotransferases (ATs, EC 2.6.1.X) are pyridoxal 5'-phosphate (PLP)-dependent enzymes, a class representing about 4% of all enzyme activities [94]. PLP is a cofactor derived from vitamin B6, involved in a wide variety of enzymatic reactions, such as decarboxylation, deamination, racemization, and transamination [95,96]. PLP-dependent enzymes are involved in crucial metabolic pathways, especially related to amino acid metabolism, in almost all living organisms. Interestingly, all ATs show a conserved lysine residue in the active site involved in PLP binding; see below.

Based on their fold, PLP-dependent enzymes have been classified into seven different groups named fold type I–VII [95], which encompass the original five fold types [97,98] with the addition of a fold type VI cluster (containing D-lysine-5,6-aminomutase) and a fold type VII cluster (including lysine-2,3-aminomutase) [95]. Only cluster V does not contain enzymes involved in amino acid metabolism [99]. Enzymes belonging to different fold groups differ in the spatial organization of the active site and cofactor orientation. ATs represent the most abundant cluster of PLP-dependent enzymes, catalysing the reversible transfer of an amino group from an amino acid to an α -ketoacid through a ping-pong mechanism.

Concerning the reaction mechanism, a Schiff base, referred to as aldimine, is formed between the ϵ -amino group of the lysine residue and the aldehyde group of PLP. After substrate binding, the following reaction involves the breakup of the internal aldimine, and a new Schiff base (external aldimine) is formed via a *gem*-diamine unstable intermediate between the aldehyde group of PLP and the amino group of the substrate via a reaction commonly named transaldimination [96] (Figure 7A). The subsequent reaction mechanism is dictated by the active site conformation and by the biochemical properties of the active site residues interacting with the external aldimine. Actually, after external aldimine formation, the following reaction is a stereospecific 1,3-proton transfer catalysed by the ϵ -amino group of the lysine residue by a common-base catalysis mechanism. The proton transfer is a two-step reaction: the deprotonation at α C leads to a carbanionic intermediate (one of its resonance forms is called “quinonoid intermediate”) [100,101]. Then, the proton is transferred from the ϵ -amino group of the lysine residue to the C4' atom of PLP, leading to a ketimine intermediate, and one water molecule is added at the C=N double bond with the formation of the carbinolamine, followed by the release of the ketoacid and of the pyridoxamine-5'-phosphate (PMP) form of the cofactor. The following half-reaction proceeds in reverse order via the formation of the new amino acid and the regeneration of PLP (Figure 7A). In this commonly accepted reaction mechanism, the proton transfer was suggested to be promoted by the conserved lysine residue involved in the formation of internal aldimine.

Amino acid transferases (AATs) are members of the fold types I (i.e., L-aspartate aminotransferase superfamily, L-Asp-ATs, EC 2.6.1.1) and IV (i.e., D-amino acid aminotransferases, D-AATs, EC 2.6.1.21, and branched-chain amino acid ATs, BCATs, EC 2.6.1.42), acting on both L- and D-amino acids [102]. L-AATs are widely exploited in the synthesis of optically pure amines and unnatural amino acids, and in the stereoselective amination of organic compounds [103,104]. D-AATs are less investigated, but their crucial role in the metabolism of D-amino acids has recently attracted attention. In bacteria, D-amino acids are involved in peptidoglycan metabolism and biofilm formation/stability as an adaptive mechanism to various environments [105–107]. Free D-amino acids also affect sporulation, bacterial communities, and gene expression [108–110]. Recent studies have demonstrated that bacterial D-amino acids including D-Trp, D-Leu, D-Phe, and D-Ser impact host–bacteria interactions [111–113]. Some bacteria such as *Bacillus sp. YM-1*, *Bacillus sphaericus*, *Rhodobacter sp. 140A*, and *Thermotoga maritima* express a D-AAT, which catalyses a transamination reaction for D-amino acid production [114]. D-AAT is the only AT active on D-amino acids and is fundamental to producing D-Ala and D-Glu for the bacterial cell wall.

Transamination is a stereoselective process: interestingly, D-AAT binds the D-amino acid to form an external aldimine with the same orientation of the α -amino and α -carboxyl groups relative to the orientation of the PLP ring observed in the complex between L-Asp-ATs and L-amino acids, while the side-chain orientation is different due to the inversion of chirality at the α C of the substrate. This difference, as well as the side chain direction of the catalytic lysine (Lys145 in D-AAT and Lys258 in L-Asp-ATs), would directly determine the strict discrimination of L- vs. D-amino acids as substrates [115].

In the reaction mechanism, the C α -H bond of the amino acid is oriented perpendicular to the π -electron plane of the PLP cofactor, either on a *re*-face or on a *si*-face of the substrate–cofactor complex (Figure 7B) [116]. Therefore, the abstraction and transfer of protons can occur stereospecifically. In particular, in the fold type I (S)-selective AATs, the proton transfer occurs on the *si*-face of the cofactor, while in class IV (including D-AATs and BCATs) it occurs on the *re*-face of the cofactor [117] (Figure 7B): the stereochemistry of the hydrogen transfer reaction is determined by the spatial arrangement of the catalytic lysine residue and the PLP cofactor [118]. In the reaction catalysed by L-Asp-ATs, Lys258 faces the side of the substrate where the α H is located, so an L-amino acid results when the reaction goes in the reverse direction (Figure 7B). Of note, BCATs are the only AATs exhibiting (S)-selectivity, with a proton transfer mechanism specific for the *re*-face-. D-AATs and BCATs share 28%

of identity, showing the conservation of key residues for the interaction with the cofactor (i.e., Lys145, Glu177 interacting with the pyridoxal nitrogen, Ile204, Thr205, Thr241, and Arg50 interacting with the phosphate group; the amino acidic numbering refers to D-AATs), in agreement with the large evolutionary conservation of the mode of PLP binding. For this reason, the selection between substrates of D- and L- configuration is performed at the substrate level: an L-amino acid must interact with BCAT in the opposite orientation compared to the interaction between a D-amino acid and D-AAT. The unique feature of BCATs is represented by a different α -carboxylate recognition site: the α -COOH group of the substrate is bound on the phosphate site of the active site, while in L-Asp-ATs and D-AATs (i.e., fold type I and IV members, respectively), the phosphate group of PLP and the α -COOH group of the substrate are separated in the active site [119,120]. Indeed, the R98 residue of D-AAT which interacts with the D-Ala carboxylic group is a methionine in BCAT.

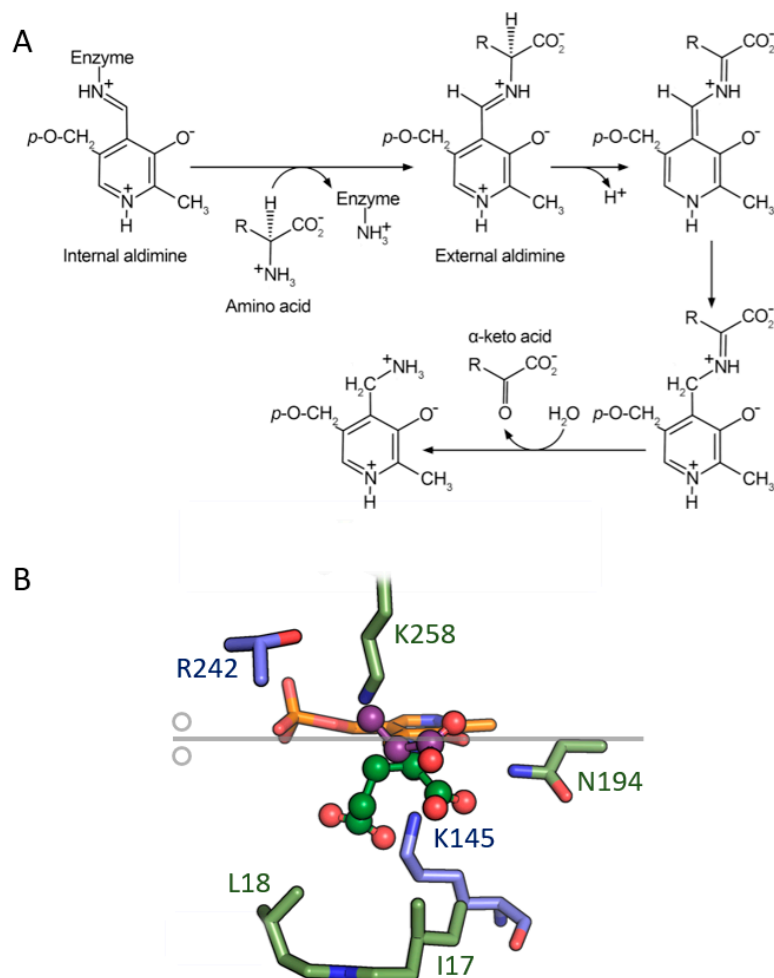


Figure 7. Symmetric arrangement of the active site of L-aspartate aminotransferase from *Gallus gallus* (variant K258H, PDB code 1AKC) and D-amino acid aminotransferase from *Bacillus* sp. (PDB code 2DAA). (A) First half of the reaction catalysed by ATs. (B) Superimposition of the structure of L-aspartate aminotransferase (green) and D-amino acid aminotransferase (blue). The PLP is depicted in yellow. The grey horizontal line represents the symmetry axis coincident with the PLP aromatic ring. Lys258 of L-aspartate aminotransferase (modelled based on His258 in the structure 1AKC) prevents the binding of D-amino acids while, similarly, Lys145 of D-amino acid aminotransferase prevents the binding of L-amino acids due to potential steric clashes with the amino acid side chains.

5. Conclusions

The key roles played by amino acids as energy sources, protein components, biological building blocks, and neuromodulators (in mammals) drove nature to evolve enzymes able to distinguish between L- and D-amino acids. The efficient oxidation/deamination/transamination of amino acids is frequently achieved through the transfer of a hydrogen atom (as a hydride ion or a proton). This catalytic strategy implies very strict geometrical requirements of the active site geometry to allow the correct interaction with the cofactors involved in the catalysis (e.g., FAD/FMN, NADP⁺, PLP). The ability to distinguish enantiomers of amino acids while retaining very efficient catalysis has been accomplished through: i) the insertion of a limited number of substitutions on a shared scaffold (e.g., LAOs vs. DAOs), i.e., starting from a common ancestral protein by divergent evolution (Figure 8A), or ii) the generation of similar active sites starting from different scaffolds by convergent evolution (Figure 8B). These processes can be considered as a remarkable example of the power of natural evolution/selection to shape the course of biological functions and processes, and in both cases, the result was the evolution of active site architectures of enzymes active on different enantiomers representing mirror images (Figure 8C).

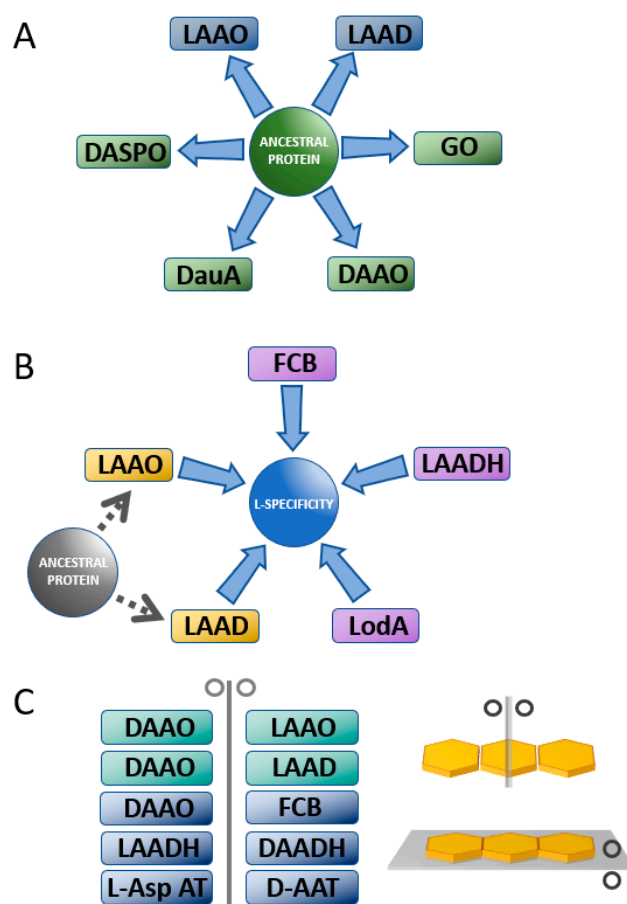


Figure 8. Schematic representation of the evolution of AAOs/AADHs. (A) Divergent evolution of AAOs/AADHs from a common ancestral protein. Blue boxes identify the acquisition of inverse enantiospecificity. (B) Convergent evolution of AAOs/AADHs toward enzymes showing a strict enantiospecificity for L-amino acids. Yellow boxes identify enzymes deriving from a common ancestor through divergent evolution (see panel A). (C) Active sites of enzymes linked by mirror symmetry. Green boxes identify mirror symmetry between enzyme pairs with the mirror plane perpendicular to the FAD cofactor; blue boxes identify mirror symmetry between enzyme pairs with the mirror plane coplanar the FAD/NADP⁺ cofactor.

Author Contributions: G.M. participated in conceptualization and original draft preparation; E.R., L.P. and G.M. participated in review and editing. All authors have read and agreed to the published version of the manuscript.

Funding: This research was partially supported by project PRIN 2020K53E57 to LP.

Data Availability Statement: Not applicable.

Acknowledgments: E.R., L.P. and G.M. thank the support of Fondo di Ateneo per la Ricerca and CIB, Consorzio Interuniversitario per le Biotecnologie.

Conflicts of Interest: The authors declare no conflict of interest.

References

1. Gal, J. Pasteur and the Art of Chirality. *Nat. Chem.* **2017**, *9*, 604–605. [[CrossRef](#)]
2. Pasteur, L. Recherches Sur Les Relations Qui Peuvent Exister Entre La Forme Cristalline, La Composition Chimique et Le Sens de La Polarisation Rotatoire. *Ann. Chim. Phys.* **1848**, *24*, 422–459.
3. Fischer, E. Über Die Konfiguration Des Traubenzuckers Und Seiner Isomeren, I & II. *Ber. Dtsch. Chem. Ges.* **1891**, *24*, 2683–2687.
4. Peretó, J.; López-García, P.; Moreira, D. Ancestral Lipid Biosynthesis and Early Membrane Evolution. *Trends Biochem. Sci.* **2004**, *29*, 469–477. [[CrossRef](#)] [[PubMed](#)]
5. Gutiérrez-Preciado, A.; Romero, H.; Peimbert, M. An Evolutionary Perspective on Amino Acids. *Nat. Educ.* **2010**, *3*, 29.
6. Sanchez, Z.; Tani, A.; Kimbara, K. Extensive Reduction of Cell Viability and Enhanced Matrix Production in *Pseudomonas Aeruginosa* PAO1 Flow Biofilms Treated with a D-Amino Acid Mixture. *Appl. Environ. Microbiol.* **2013**, *79*, 1396–1399. [[CrossRef](#)] [[PubMed](#)]
7. Hochbaum, A.I.; Kolodkin-Gal, I.; Foulston, L.; Kolter, R.; Aizenberg, J.; Losick, R. Inhibitory Effects of D-Amino Acids on *Staphylococcus Aureus* Biofilm Development. *J. Bacteriol.* **2011**, *193*, 5616–5622. [[CrossRef](#)] [[PubMed](#)]
8. Leiman, S.A.; May, J.M.; Lebar, M.D.; Kahne, D.; Kolter, R.; Losick, R. D-Amino Acids Indirectly Inhibit Biofilm Formation in *Bacillus Subtilis* by Interfering with Protein Synthesis. *J. Bacteriol.* **2013**, *195*, 5391–5395. [[CrossRef](#)]
9. Osborn, M.J. Structure and Biosynthesis of the Bacterial Cell Wall. *Annu. Rev. Biochem.* **1969**, *38*, 501–538. [[CrossRef](#)]
10. Schell, M.J.; Brady, R.O., Jr.; Molliver, M.E.; Snyder, S.H. D-Serine as a Neuromodulator: Regional and Developmental Localizations in Rat Brain Glia Resemble NMDA Receptors. *J. Neurosci.* **1997**, *17*, 1604–1615. [[CrossRef](#)]
11. Pollegioni, L.; Sacchi, S. Metabolism of the Neuromodulator D-serine. *Cell Mol. Life Sci.* **2010**, *67*, 2387–2404. [[CrossRef](#)] [[PubMed](#)]
12. Di Fiore, M.M.; Santillo, A.; Chieffi Baccari, G. Current Knowledge of D-aspartate in Glandular Tissues. *Amino Acids* **2014**, *46*, 1805–1818. [[CrossRef](#)]
13. Marcone, G.L.; Rosini, E.; Crespi, E.; Pollegioni, L. D-Amino Acids in Foods. *Appl. Microbiol. Biotechnol.* **2020**, *104*, 555–574. [[CrossRef](#)]
14. Gordon, E.M.; Ondetti, M.A.; Pluscec, J.; Cimarusti, C.M.; Bonner, D.P.; Sykes, R.B. O-Sulfated. Beta.-Lactam Hydroxamic Acids (Monosulfactams). Novel Monocyclic. Beta.-Lactam Antibiotics of Synthetic Origin. *J. Am. Chem. Soc.* **1982**, *104*, 6053–6060. [[CrossRef](#)]
15. Patel, R. Biocatalytic Synthesis of Chiral Alcohols and Amino Acids for Development of Pharmaceuticals. *Biomolecules* **2013**, *3*, 741–777. [[CrossRef](#)]
16. Gustafsson, D.; Elg, M.; Lenfors, S.; Brjesson, I.; Teger-Nilsson, A.-C. Effects of Inogatran, a New Low-Molecular-Weight Thrombin Inhibitor, in Rat Models of Venous and Arterial Thrombosis, Thrombolysis and Bleeding Time. *Blood Coagul. Fibrinolysis* **1996**, *7*, 69–79. [[CrossRef](#)]
17. Pollegioni, L.; Rosini, E.; Molla, G. Advances in Enzymatic Synthesis of D-Amino Acids. *Int. J. Mol. Sci.* **2020**, *21*, 3206. [[CrossRef](#)] [[PubMed](#)]
18. Coelho, M.M.; Fernandes, C.; Remião, F.; Tiritan, M.E. Enantioselectivity in Drug Pharmacokinetics and Toxicity: Pharmacological Relevance and Analytical Methods. *Molecules* **2021**, *26*, 3113. [[CrossRef](#)]
19. Shen, Z.; Lv, C.; Zeng, S. Significance and Challenges of Stereoselectivity Assessing Methods in Drug Metabolism. *J. Pharm. Anal.* **2016**, *6*, 1–10. [[CrossRef](#)]
20. Leek, H.; Andersson, S. Preparative Scale Resolution of Enantiomers Enables Accelerated Drug Discovery and Development. *Molecules* **2017**, *22*, 158. [[CrossRef](#)]
21. Easson, L.H.; Stedman, E. Studies on the Relationship between Chemical Constitution and Physiological Action. *Biochem. J.* **1933**, *27*, 1257–1266. [[CrossRef](#)]
22. Mikhael, S.; Abrol, R. Chiral Graphs: Reduced Representations of Ligand Scaffolds for Stereoselective Biomolecular Recognition, Drug Design, and Enhanced Exploration of Chemical Structure Space. *ChemMedChem* **2019**, *14*, 798–809. [[CrossRef](#)] [[PubMed](#)]
23. Mesecar, A.D.; Koshland, D.E. A New Model for Protein Stereospecificity. *Nature* **2000**, *403*, 614–615. [[CrossRef](#)] [[PubMed](#)]
24. Hanson, K.R. Phenylalanine Ammonia-Lyase: Mirror-Image Packing of D- and L-Phenylalanine and D- and L-Transition State Analogs into the Active Site. *Arch. Biochem. Biophys.* **1981**, *211*, 575–588. [[CrossRef](#)] [[PubMed](#)]
25. Bearne, S.L. Through the Looking Glass: Chiral Recognition of Substrates and Products at the Active Sites of Racemases and Epimerases. *Chem. A Eur. J.* **2020**, *26*, 10367–10390. [[CrossRef](#)]

26. Bentley, R. Diastereoisomerism, Contact Points, and Chiral Selectivity: A Four-Site Saga. *Arch. Biochem. Biophys.* **2003**, *414*, 1–12. [[CrossRef](#)] [[PubMed](#)]
27. Sheng, X.; Kazemi, M.; Planas, F.; Himo, F. Modeling Enzymatic Enantioselectivity using Quantum Chemical Methodology. *ACS Catal.* **2020**, *10*, 6430–6449. [[CrossRef](#)]
28. Thamim, M.; Thirumoorthy, K. Chiral Discrimination in a Mutated IDH Enzymatic Reaction in Cancer: A Computational Perspective. *Eur. Biophys. J.* **2020**, *49*, 549–559. [[CrossRef](#)]
29. Wakamatsu, T.; Sakuraba, H.; Kitamura, M.; Hakumai, Y.; Fukui, K.; Ohnishi, K.; Ashiuchi, M.; Ohshima, T. Structural Insights into L-Tryptophan Dehydrogenase from a Photoautotrophic Cyanobacterium, *Nostoc Punctiforme*. *Appl. Environ. Microbiol.* **2017**, *83*, 16. [[CrossRef](#)]
30. Li, C.; Lu, C.D. Arginine Racemization by Coupled Catabolic and Anabolic Dehydrogenases. *Proc. Natl. Acad. Sci. USA* **2009**, *106*, 906–911. [[CrossRef](#)]
31. Pollegioni, L.; Motta, P.; Molla, G. L-Amino Acid Oxidase as Biocatalyst: A Dream Too Far? *Appl. Microbiol. Biotechnol.* **2013**, *97*, 9323–9341. [[CrossRef](#)] [[PubMed](#)]
32. Lucas-Elío, P.; Gómez, D.; Solano, F.; Sanchez-Amat, A. The Antimicrobial Activity of Marinocine, Synthesized by *Marinomonas Mediterranea*, Is Due to Hydrogen Peroxide Generated by Its Lysine Oxidase Activity. *J. Bacteriol.* **2006**, *188*, 2493–2501. [[CrossRef](#)]
33. Gómez, D.; Lucas-Elío, P.; Sanchez-Amat, A.; Solano, F. A Novel Type of Lysine Oxidase: L-Lysine- ϵ -Oxidase. *Biochim. Et Biophys. Acta (BBA) Proteins Proteom.* **2006**, *1764*, 1577–1585. [[CrossRef](#)] [[PubMed](#)]
34. Schriek, S.; Kahmann, U.; Staiger, D.; Pistorius, E.K.; Michel, K.-P. Detection of an L-Amino Acid Dehydrogenase Activity in *Synechocystis* Sp. PCC 6803. *J. Exp. Bot.* **2009**, *60*, 1035–1046. [[CrossRef](#)] [[PubMed](#)]
35. Krebs, H.A. Metabolism of Amino-Acids. *Biochem. J.* **1935**, *29*, 1951–1969. [[CrossRef](#)]
36. Mattevi, A.; Vanoni, M.A.; Todone, F.; Rizzi, M.; Teplyakov, A.; Coda, A.; Bolognesi, M.; Curti, B. Crystal Structure of D-Amino Acid Oxidase: A Case of Active Site Mirror-Image Convergent Evolution with Flavocytochrome B2. *Proc. Natl. Acad. Sci. USA* **1996**, *93*, 7496–7501. [[CrossRef](#)]
37. Pilone, M.S.; Pollegioni, L. D-Amino Acid Oxidase as an Industrial Biocatalyst. *Biocatal. Biotransformation* **2002**, *20*, 145–159. [[CrossRef](#)]
38. Job, V.; Molla, G.; Pilone, M.S.; Pollegioni, L. Overexpression of a Recombinant Wild-Type and His-Tagged *Bacillus Subtilis* Glycine Oxidase in *Escherichia Coli*. *Eur. J. Biochem.* **2002**, *269*, 1456–1463. [[CrossRef](#)]
39. Job, V.; Marcone, G.L.; Pilone, M.S.; Pollegioni, L. Glycine Oxidase from *Bacillus Subtilis*. Characterization of a New Flavoprotein. *J. Biol. Chem.* **2002**, *277*, 6985–6993. [[CrossRef](#)]
40. Mörtl, M.; Diederichs, K.; Welte, W.; Molla, G.; Motteran, L.; Andriolo, G.; Pilone, M.S.; Pollegioni, L. Structure-Function Correlation in Glycine Oxidase from *Bacillus Subtilis*. *J. Biol. Chem.* **2004**, *279*, 29718–29727. [[CrossRef](#)]
41. Settembre, E.; Begley, T.P.; Ealick, S.E. Structural Biology of Enzymes of the Thiamin Biosynthesis Pathway. *Curr. Opin. Struct. Biol.* **2003**, *13*, 739–747. [[CrossRef](#)] [[PubMed](#)]
42. Umhau, S.; Pollegioni, L.; Molla, G.; Diederichs, K.; Welte, W.; Pilone, M.S.; Ghisla, S. The X-Ray Structure of D-Amino Acid Oxidase at Very High Resolution Identifies the Chemical Mechanism of Flavin-Dependent Substrate Dehydrogenation. *Proc. Natl. Acad. Sci. USA* **2000**, *97*, 12463–12468. [[CrossRef](#)] [[PubMed](#)]
43. Pollegioni, L.; Piubelli, L.; Sacchi, S.; Pilone, M.S.; Molla, G. Physiological Functions of D-Amino Acid Oxidases: From Yeast to Humans. *Cell. Mol. Life Sci.* **2007**, *64*, 1373–1394. [[CrossRef](#)] [[PubMed](#)]
44. Pawelek, P.D.; Cheah, J.; Coulombe, R.; Macheroux, P.; Ghisla, S.; Vrieland, A. The Structure of L-Amino Acid Oxidase Reveals the Substrate Trajectory into an Enantiomerically Conserved Active Site. *EMBO J.* **2000**, *19*, 4204–4215. [[CrossRef](#)]
45. Yu, Z.; Qiao, H. Advances in Non-Snake Venom L-Amino Acid Oxidase. *Appl. Biochem. Biotechnol.* **2012**, *167*, 1–13. [[CrossRef](#)]
46. Lukashcheva, E.V.; Efremova, A.A.; Treshalina, E.M.; Arinbasarova, A.Y.; Medentzev, A.G.; Berezov, T.T. L-Amino Acid Oxidases: Properties and Molecular Mechanisms of Action. *Biochem. Mosc. Suppl. B Biomed. Chem.* **2011**, *5*, 337–345. [[CrossRef](#)]
47. Izidoro, L.F.M.; Sobrinho, J.C.; Mendes, M.M.; Costa, T.R.; Grabner, A.N.; Rodrigues, V.M.; da Silva, S.L.; Zanchi, F.B.; Zuliani, J.P.; Fernandes, C.F.C.; et al. Snake Venom L-Amino Acid Oxidases: Trends in Pharmacology and Biochemistry. *Biomed. Res. Int.* **2014**, *2014*, 196754. [[CrossRef](#)]
48. Nielsen, V.G. Characterization of L-Amino Acid Oxidase Derived from *Crotalus Adamanteus* Venom: Procoagulant and Anticoagulant Activities. *Int. J. Mol. Sci.* **2019**, *20*, 4853. [[CrossRef](#)]
49. Yang, C.A.; Cheng, C.H.; Lo, C.T.; Liu, S.Y.; Lee, J.W.; Peng, K.C. A Novel L-Amino Acid Oxidase from *Trichoderma Harzianum* ETS 323 Associated with Antagonism of *Rhizoctonia Solani*. *J. Agric. Food Chem.* **2011**, *59*, 4519–4526. [[CrossRef](#)]
50. Mai-Prochnow, A.; Lucas-Elío, P.; Egan, S.; Thomas, T.; Webb, J.S.; Sanchez-Amat, A.; Kjelleberg, S. Hydrogen Peroxide Linked to Lysine Oxidase Activity Facilitates Biofilm Differentiation and Dispersal in Several Gram-Negative Bacteria. *J. Bacteriol.* **2008**, *190*, 5493–5501. [[CrossRef](#)]
51. Kitani, Y.; Kikuchi, N.; Zhang, G.; Ishizaki, S.; Shimakura, K.; Shiomi, K.; Nagashima, Y. Antibacterial Action of L-Amino Acid Oxidase from the Skin Mucus of Rockfish *Sebastes Schlegelii*. *Comp. Biochem. Physiol. B Biochem. Mol. Biol.* **2008**, *149*, 394–400. [[CrossRef](#)] [[PubMed](#)]
52. Kasai, K.; Ishikawa, T.; Nakamura, T.; Miura, T. Antibacterial Properties of L-Amino Acid Oxidase: Mechanisms of Action and Perspectives for Therapeutic Applications. *Appl. Microbiol. Biotechnol.* **2015**, *99*, 7847–7857. [[CrossRef](#)] [[PubMed](#)]

53. Puiffe, M.-L.; Lachaise, I.; Molinier-Frenkel, V.; Castellano, F. Antibacterial Properties of the Mammalian L-Amino Acid Oxidase IL4I1. *PLoS ONE* **2013**, *8*, e54589. [[CrossRef](#)] [[PubMed](#)]
54. Saam, J.; Rosini, E.; Molla, G.; Schulten, K.; Pollegioni, L.; Ghisla, S. O₂ Reactivity of Flavoproteins: Dynamic Access of Dioxygen to the Active Site and Role of a H⁺ Relay System in D-Amino Acid Oxidase. *J. Biol. Chem.* **2010**, *285*, 24439–24446. [[CrossRef](#)] [[PubMed](#)]
55. Ball, J.; Gannavaram, S.; Gadda, G. Structural Determinants for Substrate Specificity of Flavoenzymes Oxidizing D-Amino Acids. *Arch. Biochem. Biophys.* **2018**, *660*, 87–96. [[CrossRef](#)] [[PubMed](#)]
56. Molla, G.; Porrini, D.; Job, V.; Motteran, L.; Vegezzi, C.; Campaner, S.; Pilone, M.S.; Pollegioni, L. Role of Arginine 285 in the Active Site of *Rhodotorula gracilis* D-amino Acid Oxidase. A Site-Directed Mutagenesis Study. *J. Biol. Chem.* **2000**, *275*, 24715–24721. [[CrossRef](#)]
57. Kawazoe, T.; Park, H.K.; Iwana, S.; Tsuge, H.; Fukui, K. Human D-Amino Acid Oxidase: An Update and Review. *Chem. Rec.* **2007**, *7*, 305–315. [[CrossRef](#)]
58. Liu, Q.; Chen, L.; Zhang, Z.; Du, B.; Xiao, Y.; Yang, K.; Gong, L.; Wu, L.; Li, X.; He, Y. pH-Dependent Enantioselectivity of D-Amino Acid Oxidase in Aqueous Solution. *Sci. Rep.* **2017**, *7*, 2994. [[CrossRef](#)]
59. Pollegioni, L.; Diederichs, K.; Molla, G.; Umhau, S.; Welte, W.; Ghisla, S.; Pilone, M.S. Yeast D-Amino Acid Oxidase: Structural Basis of Its Catalytic Properties. *J. Mol. Biol.* **2002**, *324*, 535–546. [[CrossRef](#)]
60. Takahashi, S.; Takahashi, T.; Kera, Y.; Matsunaga, R.; Shibuya, H.; Yamada, R.H. Cloning and Expression in *Escherichia Coli* of the D-Aspartate Oxidase Gene from the Yeast *Cryptococcus Humicola* and Characterization of the Recombinant Enzyme. *J. Biochem.* **2004**, *135*, 533–540. [[CrossRef](#)]
61. Negri, A.; Cecilian, F.; Tedeschi, G.; Simonic, T.; Ronchi, S. The Primary Structure of the Flavoprotein D-Aspartate Oxidase from Beef Kidney. *J. Biol. Chem.* **1992**, *267*, 11865–11871. [[CrossRef](#)] [[PubMed](#)]
62. Takahashi, S.; Kakuichi, T.; Fujii, K.; Kera, Y.; Yamada, R. Physiological Role Of D-Aspartate Oxidase in the Assimilation and Detoxification Of D-Aspartate in the Yeast *Cryptococcus Humicola*. *Yeast* **2005**, *22*, 1203–1212. [[CrossRef](#)] [[PubMed](#)]
63. Saitoh, Y.; Katane, M.; Miyamoto, T.; Sekine, M.; Sakamoto, T.; Imai, H.; Homma, H. Secreted D-Aspartate Oxidase Functions in *C. Elegans* Reproduction and Development. *FEBS J.* **2019**, *286*, 124–138. [[CrossRef](#)]
64. Molla, G.; Chaves-Sanjuan, A.; Savinelli, A.; Nardini, M.; Pollegioni, L. Structure and Kinetic Properties of Human D-Aspartate Oxidase, the Enzyme-Controlling d-Aspartate Levels in Brain. *FASEB J.* **2020**, *34*, 1182–1197. [[CrossRef](#)] [[PubMed](#)]
65. Katane, M.; Kawata, T.; Nakayama, K.; Saitoh, Y.; Kaneko, Y.; Matsuda, S.; Saitoh, Y.; Miyamoto, T.; Sekine, M.; Homma, H. Characterization of the Enzymatic and Structural Properties of Human D-Aspartate Oxidase and Comparison with Those of the Rat and Mouse Enzymes. *Biol. Pharm. Bull.* **2015**, *38*, 298–305. [[CrossRef](#)]
66. Takahashi, S. D-Aspartate Oxidase: Distribution, Functions, Properties, and Biotechnological Applications. *Appl. Microbiol. Biotechnol.* **2020**, *104*, 2883–2895. [[CrossRef](#)]
67. Tedeschi, G.; Negri, A.; Mortarino, M.; Cecilian, F.; Simonic, T.; Faotto, L.; Ronchi, S. L-Aspartate Oxidase from *Escherichia Coli*. II. Interaction with C₄ Dicarboxylic Acids and Identification of a Novel L-Aspartate:Fumarate Oxidoreductase Activity. *Eur. J. Biochem.* **1996**, *239*, 427–433. [[CrossRef](#)]
68. Motta, P.; Molla, G.; Pollegioni, L.; Nardini, M. Structure-Function Relationships in L-Amino Acid Deaminase, a Flavoprotein Belonging to a Novel Class of Biotechnologically Relevant Enzymes. *J. Biol. Chem.* **2016**, *291*, 10457–10475. [[CrossRef](#)]
69. Takahashi, E.; Ito, K.; Yoshimoto, T. Cloning of L-Amino Acid Deaminase Gene from *Proteus Vulgaris*. *Biosci. Biotechnol. Biochem.* **1999**, *63*, 2244–2247. [[CrossRef](#)]
70. Molla, G.; Melis, R.; Pollegioni, L. Breaking the Mirror: L-Amino Acid Deaminase, a Novel Stereoselective Biocatalyst. *Biotechnol. Adv.* **2017**, *35*, 657–668. [[CrossRef](#)]
71. Stefan, R.I.; Bokretsi, R.G.; van Staden, J.F.; Aboul-Enein, H.Y. Determination of L- And D-Enantiomers of Methotrexate Using Amperometric Biosensors. *Talanta* **2003**, *60*, 983–990. [[CrossRef](#)] [[PubMed](#)]
72. Inaba, Y.; Mizukami, K.; Hamada-Sato, N.; Kobayashi, T.; Imada, C.; Watanabe, E. Development of a L-Alanine Sensor for the Monitoring of a Fermentation Using the Improved Selectivity by the Combination of D-Amino Acid Oxidase and Pyruvate Oxidase. *Biosens. Bioelectron.* **2003**, *19*, 423–431. [[CrossRef](#)] [[PubMed](#)]
73. Domínguez, R.; Serra, B.; Reviejo, A.J.; Pingarrón, J.M. Chiral Analysis of Amino Acids Using Electrochemical Composite Bionzyme Biosensors. *Anal. Biochem.* **2001**, *298*, 275–282. [[CrossRef](#)] [[PubMed](#)]
74. Rosini, E.; Molla, G.; Rossetti, C.; Pilone, M.S.; Pollegioni, L.; Sacchi, S. A Biosensor for All D-Amino Acids Using Evolved D-Amino Acid Oxidase. *J. Biotechnol.* **2008**, *135*, 377–384. [[CrossRef](#)] [[PubMed](#)]
75. Pernot, P.; Mothet, J.P.; Schuvailo, O.; Soldatkin, A.; Pollegioni, L.; Pilone, M.; Adeline, M.T.; Cespuglio, R.; Marinesco, S. Characterization of a Yeast D-Amino Acid Oxidase Microbiosensor for D-Serine Detection in the Central Nervous System. *Anal. Chem.* **2008**, *80*, 1589–1597. [[CrossRef](#)]
76. Pollegioni, L.; Molla, G. New Biotech Applications from Evolved D-Amino Acid Oxidases. *Trends Biotechnol.* **2011**, *29*, 276–283. [[CrossRef](#)]
77. Melis, R.; Rosini, E.; Pirillo, V.; Pollegioni, L.; Molla, G. In Vitro Evolution of an L-Amino Acid Deaminase Active on L-1-Naphthylalanine. *Catal. Sci. Technol.* **2018**, *8*, 5359–5367. [[CrossRef](#)]
78. Moynihan, K.; Elion, G.B.; Pegram, C.; Reist, C.J.; Wellner, D.; Bigner, D.D.; Griffith, O.W.; Friedman, H.S. L -Amino Acid Oxidase (LOX) Modulation of Methylglucosyltransferase Activity against Intracranial Glioma. *Cancer Chemother. Pharmacol.* **1996**, *39*, 179–186. [[CrossRef](#)]

79. Lukasheva, E.V.; Berezov, T.T. L-Lysine Alpha-Oxidase: Physicochemical and Biological Properties. *Biochemistry* **2002**, *67*, 1152–1158. [[CrossRef](#)]
80. Sukhacheva, M.V.; Zhuravleva, N.I. Properties and Prospects of Practical Use of Extracellular L-Glutamate Oxidase from *Streptomyces* Sp. Z-11-6. *Prikl. Biokhim. Mikrobiol.* **2004**, *40*, 173–177.
81. Gherardini, P.F.; Wass, M.N.; Helmer-Citterich, M.; Sternberg, M.J.E. Convergent Evolution of Enzyme Active Sites Is Not a Rare Phenomenon. *J. Mol. Biol.* **2007**, *372*, 817–845. [[CrossRef](#)] [[PubMed](#)]
82. Ogura, R.; Wakamatsu, T.; Mutaguchi, Y.; Doi, K.; Ohshima, T. Biochemical Characterization of an L-Tryptophan Dehydrogenase from the Photoautotrophic Cyanobacterium *Nostoc Punctiforme*. *Enzyme Microb. Technol.* **2014**, *60*, 40–46. [[CrossRef](#)] [[PubMed](#)]
83. Baker, P.J.; Waugh, M.L.; Wang, X.-G.; Stillman, T.J.; Turnbull, A.P.; Engel, P.C.; Rice, D.W. Determinants of Substrate Specificity in the Superfamily of Amino Acid Dehydrogenases. *Biochemistry* **1997**, *36*, 16109–16115. [[CrossRef](#)]
84. Britton, K.L.; Baker, P.J.; Engel, P.C.; Rice, D.W.; Stillman, T.J. Evolution of Substrate Diversity in the Superfamily of Amino Acid Dehydrogenases. *J. Mol. Biol.* **1993**, *234*, 938–945. [[CrossRef](#)]
85. Heydari, M.; Ohshima, T.; Nunoura-Kominato, N.; Sakuraba, H. Highly Stable L-Lysine 6-Dehydrogenase from the Thermophile *Geobacillus Stearothermophilus* Isolated from a Japanese Hot Spring: Characterization, Gene Cloning and Sequencing, and Expression. *Appl. Environ. Microbiol.* **2004**, *70*, 937–942. [[CrossRef](#)] [[PubMed](#)]
86. Zhou, X.; Liu, Q.; Wang, H. Chiral Resolution of DL-glutamic Acid by a Chiral Additive. *J. Chem. Technol. Biotechnol.* **2022**, *97*, 1240–1246. [[CrossRef](#)]
87. Son, H.F.; Kim, I.K.; Kim, K.J. Structural Insights into Domain Movement and Cofactor Specificity of Glutamate Dehydrogenase from *Corynebacterium Glutamicum*. *Biochem. Biophys. Res. Commun.* **2015**, *459*, 387–392. [[CrossRef](#)]
88. Tomita, T.; Yin, L.; Nakamura, S.; Kosono, S.; Kuzuyama, T.; Nishiyama, M. Crystal Structure of the 2-Iminoglutarate-Bound Complex of Glutamate Dehydrogenase from *Corynebacterium Glutamicum*. *FEBS Lett.* **2017**, *591*, 1611–1622. [[CrossRef](#)]
89. Jones, H.; Venables, W.A. Effects of Solubilisation on Some Properties of the Membrane-Bound Respiratory Enzyme D-Amino Acid Dehydrogenase of *Escherichia Coli*. *FEBS Lett.* **1983**, *151*, 189–192. [[CrossRef](#)]
90. Olsiewski, P.J.; Kaczorowski, G.J.; Walsh, C. Purification and Properties of D-Amino Acid Dehydrogenase, an Inducible Membrane-Bound Iron-Sulfur Flavoenzyme from *Escherichia Coli* B. *J. Biol. Chem.* **1980**, *255*, 4487–4494. [[CrossRef](#)]
91. Xu, J.; Bai, Y.; Fan, T.; Zheng, X.; Cai, Y. Expression, Purification, and Characterization of a Membrane-Bound D-Amino Acid Dehydrogenase from *Proteus Mirabilis* JN458. *Biotechnol. Lett.* **2017**, *39*, 1559–1566. [[CrossRef](#)] [[PubMed](#)]
92. Todone, F.; Vanoni, M.A.; Mozzarelli, A.; Bolognesi, M.; Coda, A.; Curti, B.; Mattevi, A. Active Site Plasticity in D-Amino Acid Oxidase: A Crystallographic Analysis. *Biochemistry* **1997**, *36*, 5853–5860. [[CrossRef](#)] [[PubMed](#)]
93. Ouedraogo, D.; Souffrant, M.; Vasquez, S.; Hamelberg, D.; Gadda, G. Importance of Loop L1 Dynamics for Substrate Capture and Catalysis in *Pseudomonas Aeruginosa* D-Arginine Dehydrogenase. *Biochemistry* **2017**, *56*, 2477–2487. [[CrossRef](#)] [[PubMed](#)]
94. Clausen, T.; Huber, R.; Laber, B.; Pohlenz, H.-D.; Messerschmidt, A. Crystal Structure of the Pyridoxal-5'-Phosphate Dependent Cystathionine β -Lyase From *Escherichia Coli* at 1.83 Å. *J. Mol. Biol.* **1996**, *262*, 202–224. [[CrossRef](#)]
95. Percudani, R.; Peracchi, A. The B6 Database: A Tool for the Description and Classification of Vitamin B6-Dependent Enzymatic Activities and of the Corresponding Protein Families. *BMC Bioinform.* **2009**, *10*, 273. [[CrossRef](#)]
96. Liang, J.; Han, Q.; Tan, Y.; Ding, H.; Li, J. Current Advances on Structure-Function Relationships of Pyridoxal 5'-Phosphate-Dependent Enzymes. *Front. Mol. Biosci.* **2019**, *6*, 4. [[CrossRef](#)]
97. Grishin, N.V.; Phillips, M.A.; Goldsmith, E.J. Modeling of the Spatial Structure of Eukaryotic Ornithine Decarboxylases. *Protein Sci.* **1995**, *4*, 1291–1304. [[CrossRef](#)]
98. Schneider, G.; Käck, H.; Lindqvist, Y. The Manifold of Vitamin B6 Dependent Enzymes. *Structure* **2000**, *8*, R1–R6. [[CrossRef](#)]
99. Yoshimura, T.; Goto, M. D-Amino Acids in the Brain: Structure and Function of Pyridoxal Phosphate-Dependent Amino Acid Racemases. *FEBS J.* **2008**, *275*, 3527–3537. [[CrossRef](#)]
100. Toney, M.D.; Kirsch, J.F. The K258R Mutant of Aspartate Aminotransferase Stabilizes the Quinonoid Intermediate. *J. Biol. Chem.* **1991**, *266*, 23900–23903. [[CrossRef](#)]
101. Toney, M.D. Controlling Reaction Specificity in Pyridoxal Phosphate Enzymes. *Biochim. Biophys. Acta (BBA)-Proteins Proteom.* **2011**, *1814*, 1407–1418. [[CrossRef](#)] [[PubMed](#)]
102. Bezsudnova, E.Y.; Popov, V.O.; Boyko, K.M. Structural Insight into the Substrate Specificity of PLP Fold Type IV Transaminases. *Appl. Microbiol. Biotechnol.* **2020**, *104*, 2343–2357. [[CrossRef](#)] [[PubMed](#)]
103. Caligiuri, A.; D'Arrigo, P.; Gefflaut, T.; Molla, G.; Pollegioni, L.; Rosini, E.; Rossi, C.; Servi, S. Multistep Enzyme Catalysed Deracemisation of 2-Naphthyl Alanine. *Biocatal. Biotransformation* **2006**, *24*, 409–413. [[CrossRef](#)]
104. Steffen-Munsberg, F.; Vickers, C.; Kohls, H.; Land, H.; Mallin, H.; Nobili, A.; Skalden, L.; van den Bergh, T.; Joosten, H.J.; Berglund, P.; et al. Bioinformatic Analysis of a PLP-Dependent Enzyme Superfamily Suitable for Biocatalytic Applications. *Biotechnol. Adv.* **2015**, *33*, 566–604. [[CrossRef](#)]
105. Yu, C.; Li, X.; Zhang, N.; Wen, D.; Liu, C.; Li, Q. Inhibition of Biofilm Formation by D-Tyrosine: Effect of Bacterial Type and D-Tyrosine Concentration. *Water Res.* **2016**, *92*, 173–179. [[CrossRef](#)]
106. Kolodkin-Gal, I.; Romero, D.; Cao, S.; Clardy, J.; Kolter, R.; Losick, R. D-Amino Acids Trigger Biofilm Disassembly. *Science* **2010**, *328*, 627–629. [[CrossRef](#)]
107. Miyamoto, T.; Homma, H. D-Amino Acid Metabolism in Bacteria. *J. Biochem.* **2021**, *170*, 5–13. [[CrossRef](#)]

108. Miyamoto, T.; Katane, M.; Saitoh, Y.; Sekine, M.; Homma, H. Involvement of Penicillin-Binding Proteins in the Metabolism of a Bacterial Peptidoglycan Containing a Non-Canonical D-Amino Acid. *Amino Acids* **2020**, *52*, 487–497. [[CrossRef](#)]
109. Li, E.; Wu, J.; Wang, P.; Zhang, D. D-Phenylalanine Inhibits Biofilm Development of a Marine Microbe, *Pseudoalteromonas* Sp. SC2014. *FEMS Microbiol. Lett.* **2016**, *363*, fnw198. [[CrossRef](#)]
110. Warraich, A.A.; Mohammed, A.R.; Perrie, Y.; Hussain, M.; Gibson, H.; Rahman, A. Evaluation of Anti-Biofilm Activity of Acidic Amino Acids and Synergy with Ciprofloxacin on *Staphylococcus Aureus* Biofilms. *Sci. Rep.* **2020**, *10*, 9021. [[CrossRef](#)]
111. Nakade, Y.; Iwata, Y.; Furuichi, K.; Mita, M.; Hamase, K.; Konno, R.; Miyake, T.; Sakai, N.; Kitajima, S.; Toyama, T.; et al. Gut Microbiota-Derived D-Serine Protects against Acute Kidney Injury. *JCI Insight* **2018**, *3*, 97957. [[CrossRef](#)] [[PubMed](#)]
112. Lee, R.J.; Hariri, B.M.; McMahon, D.B.; Chen, B.; Doghramji, L.; Adappa, N.D.; Palmer, J.N.; Kennedy, D.W.; Jiang, P.; Margolskee, R.F.; et al. Bacterial D-Amino Acids Suppress Sinus Innate Immunity through Sweet Taste Receptors in Solitary Chemosensory Cells. *Sci. Signal* **2017**, *10*, 7703. [[CrossRef](#)] [[PubMed](#)]
113. Kepert, I.; Fonseca, J.; Müller, C.; Milger, K.; Hochwind, K.; Kostric, M.; Fedoseeva, M.; Ohnmacht, C.; Dehmel, S.; Nathan, P.; et al. D-Tryptophan from Probiotic Bacteria Influences the Gut Microbiome and Allergic Airway Disease. *J. Allergy Clin. Immunol.* **2017**, *139*, 1525–1535. [[CrossRef](#)]
114. Miyamoto, T.; Moriya, T.; Katane, M.; Saitoh, Y.; Sekine, M.; Sakai-Kato, K.; Oshima, T.; Homma, H. Identification of a Novel D-amino Acid Aminotransferase Involved in D-glutamate Biosynthetic Pathways in the Hyperthermophile *Thermotoga Maritima*. *FEBS J.* **2022**, *289*, 5933–5946. [[CrossRef](#)]
115. Sugio, S.; Petsko, G.A.; Manning, J.M.; Soda, K.; Ringe, D. Crystal Structure of a D-Amino Acid Aminotransferase: How the Protein Controls Stereoselectivity. *Biochemistry* **1995**, *34*, 9661–9669. [[CrossRef](#)]
116. Dunathan, H.C. Stereochemical Aspects of Pyridoxal Phosphate Catalysis. *Adv. Enzymol. Relat. Areas Mol. Biol.* **2006**, *35*, 79–134.
117. Soda, K.; Yoshimura, T.; Esaki, N. Stereospecificity for the Hydrogen Transfer of Pyridoxal Enzyme Reactions. *Chem. Rec.* **2001**, *1*, 373–384. [[CrossRef](#)]
118. Almo, S.C.; Smith, D.L.; Danishefsky, A.T.; Ringe, D. The Structural Basis for the Altered Substrate Specificity of the R292D Active Site Mutant of Aspartate Aminotransferase from *E. coli*. *Protein Eng. Des. Sel.* **1994**, *7*, 405–412. [[CrossRef](#)]
119. Bezsudnova, E.Y.; Boyko, K.M.; Popov, V.O. Properties of Bacterial and Archaeal Branched-Chain Amino Acid Aminotransferases. *Biochemistry* **2017**, *82*, 1572–1591. [[CrossRef](#)]
120. Goto, M.; Miyahara, I.; Hayashi, H.; Kagamiyama, H.; Hirotsu, K. Crystal Structures of Branched-Chain Amino Acid Aminotransferase Complexed with Glutamate and Glutarate: True Reaction Intermediate and Double Substrate Recognition of the Enzyme. *Biochemistry* **2003**, *42*, 3725–3733. [[CrossRef](#)]

Disclaimer/Publisher’s Note: The statements, opinions and data contained in all publications are solely those of the individual author(s) and contributor(s) and not of MDPI and/or the editor(s). MDPI and/or the editor(s) disclaim responsibility for any injury to people or property resulting from any ideas, methods, instructions or products referred to in the content.